The Contribution of Lysine-36 to Catalysis by Human *myo*-Inositol Monophosphatase

Axel J. Ganzhorn,* Pierre Lepage,‡ Patricia D. Pelton,§ Françoise Strasser,|| Pascale Vincendon,⊥ and Jean-Michel Rondeau

Marion Merrell Research Institute, 16 rue d'Ankara, 67080 Strasbourg Cedex, France

Received February 16, 1996; Revised Manuscript Received May 29, 1996⊗

ABSTRACT: The role of lysine residues in the catalytic mechanism of *myo*-inositol monophosphatase (EC 3.1.3.25) was investigated. The enzyme was completely inactivated by amidination with ethyl acetimidate or reductive methylation with formaldehyde and cyanoborohydride. Activity was retained when the active site was protected with Mg^{2+}, Li^+, and D,L-*myo*-inositol 1-phosphate. Using radiolabeling, peptide mapping, and sequence analysis, Lys-36 was shown to be the protected residue, which is responsible for inactivation. Replacing Lys-36 with glutamine produced a mutant protein, K36Q, with similar affinities for the substrate and the activator Mg^{2+}, but a 50-fold lower turnover number as compared to the wild-type enzyme. Crystallographic studies did not indicate any gross structural changes in the mutant as compared to the native form. Initial velocity data were best described by a rapid equilibrium ordered mechanism with two Mg^{2+} binding before and a third one binding after the substrate. Inhibition by calcium was unaffected by the mutation, but inhibition by lithium was greatly reduced and became noncompetitive. The pH dependence of catalysis and the solvent isotope effect on k_{cat} are altered in the mutant enzyme. D,L-*myo*-Inositol 1-phosphate, 4-nitrophenyl phosphate, and D-glucose 6-phosphate are cleaved at different rates by the wild-type enzyme, but with similar efficiency by K36Q. All data taken together are consistent with the hypothesis that modifying or replacing the lysine residue in position 36 decreases its polarizing effect on one of the catalytic metal ions and prevents the efficient deprotonation of the metal-bound water nucleophile.

myo-Inositol monophosphatase (EC 3.1.3.25) catalyzes the hydrolysis of several inositol monophosphate isomers to *myo*-inositol. The reaction plays an important role in the intracellular phosphatidylinositol signaling pathways of nerve cells, since it provides the free inositol needed to replenish membrane inositol lipid pools. The enzyme is considered a potential target for drug therapy, since it is inhibited by Li^+, a metal ion that is widely used in the treatment of manic depression [for review articles, see Berridge et al. (1989), Nahorski et al. (1991), Belmaker et al. (1995), Gani et al. (1993), Jope and Williams (1994), and Parthasarathy et al. (1994)]. The enzyme is activated by Mg^{2+} in a nonlinear fashion, but uncompetitively inhibited by Li^+ and high concentrations of Mg^{2+} (Hallcher & Sherman, 1980; Ganzhorn & Chanal, 1990). The three-dimensional structure of human brain *myo*-inositol monophosphatase complexed to substrate and metal ions was recently reported (Bone et al., 1994a,b). It shows the existence of up to three metal ion binding sites formed by phosphate oxygens and several acidic active site residues. A mechanism for catalysis was proposed, where one Mg^{2+} activates a water molecule for nucleophilic attack on the phosphoester and a second Mg^{2+} stabilizes the alcoholate leaving group. The identity and precise role of active site residues, other than the direct metal ligands, that are essential for or aid in this process still need to be defined. Histidine and arginine have been discussed as important active site residues based on chemical modification experiments (Pelton & Ganzhorn, 1992; Jackson et al., 1989), but the X-ray structure and mutagenesis studies (Rees-Milton et al., 1993) have ruled out an essential function for such residues. Similarly, chemical modification of an active site cysteine (Cys-218) with bulky agents leads to inactivation, but the activity of a C218A mutant was unaltered (Knowles et al., 1992), even though it had different metal ion binding properties (Gore et al., 1993).

Based on the amino acid sequence of *myo*-inositol monophosphatase, Wreggett (1992) suggested Lys-137 to be involved in phosphate binding. The X-ray structure, however, does not support this hypothesis. Pollack et al. (1993) have substituted many of the amino acids in inositol monophosphatase that are close to the metal ion binding sites. Replacing Lys-36 with isoleucine reduced the catalytic activity and the apparent affinities for lithium and magnesium. We have used chemical modification in combination with peptide mapping experiments to characterize important lysine residues in *myo*-inositol monophosphatase. In addition, the role of Lys-36 in catalysis was further studied by site-directed mutagenesis, kinetics, and X-ray crystallography.

* To whom correspondence should be addressed. Email: AxelGanzhorn@mmd.com. Fax: (33) 88 45 90 75.

‡ Present address: Laboratoires Serono S.A., CH-1170 Aubonne, Switzerland.

§ Present address: Department of Cell Biology, Neurobiology & Anatomy, University of Cincinnati, P.O. 67052, Cincinnati, OH 45267-0251.

|| Present address: Department of Biochemistry, The University of Iowa, Iowa City, IA 52242-1109.

⊥ Present address: Innovex France S.A.R.L., 91300 Massy, France.

⊗ Abstract published in *Advance ACS Abstracts,* August 1, 1996.

S0006-2960(96)00383-2 CCC: $12.00

EXPERIMENTAL PROCEDURES

Materials. D-Glucose 6-phosphate, 4-nitrophenyl phosphate, $MgCl_2$, $CaCl_2$, ethylacetimidate, and D_2O were obtained from Sigma. Formaldehyde was from Merck and [^{14}C]formaldehyde from NEN. LiCl and $(Gd)_2(SO_4)_3$ were purchased from Aldrich, Glu-C protease from Boehringer Mannheim, and Ins(1)P[1] from Bachem. All reagents for the polymerase chain reaction were obtained from Perkin Elmer. The PCR products were purified using the Gene-Clean kit (Bio 101). Restriction enzymes, other DNA modifying enzymes, and corresponding buffers plus the vector pUC19 were from New England Biolabs. The vector pT7.6 containing the promotor for T7 RNA polymerase plus ampicillin resistance and used for expression of the mutant protein was a gift from Stan Tabor (Harvard University). All oligonucleotides were synthesized with an Applied Biosystems Model 381A DNA synthesizer using phosphoramidate chemistry. The Applied Biosystems automated DNA sequencer Model 373A and the corresponding Taq dideoxy terminator sequencing kit were used for sequencing, and the analysis was aided by the University of Wisconsin Genetic Computer Group program. The components for the growth and propagation of all the *Escherichia coli* strains were obtained from Difco (Detroit, MI) or Sigma. Isopropyl β-D-thiogalactopyranoside (IPTG) was purchased from Clonetech (Ozyme). The competent strain of *E. coli* JM109 was supplied by Stratagene. The strain for expression of the proteins was BL21(DE3)pLys S and was donated by Raymond Leppick.

Mutagenesis. The wild-type clone of human *myo*-inositol monophosphatase was obtained by RT-PCR as previously described for the bovine enzyme (Strasser et al., 1995). Oligonucleotides were based on the published sequence for the human isoform (McAllister et al., 1992). The mutant K36Q was prepared by PCR using the GeneAmp reagents (Perkin Elmer) according to the manufacturer's instructions and the technique of overlap extension (Ho et al., 1989). The following oligonucleotide primers were used: P1 (5′-GAATGTTATGCTG**C**AAAGTTCTCCAG-3′) and P2 (5′-CTGGAGAACTTT**G**CAGCATAACATTC-3′) are complementary and contain the mutant sequence as noted in boldface print. P3 (5′-**GAGCTCCTGCAG**AGGAGGAATATAAT*ATG*GC-TGATCCTT-3′) and P4 (5′-**GTCGACTCTAGA**TTAATCTTCGTCGTC-3′) flank the entire coding sequence of the human *myo*-inositol monophosphatase cDNA plus restriction sites for subcloning purposes (outlined in boldface print). P3 also contains a ribosome binding site with a spacer for prokaryotic expression (underlined) and the start codon, *ATG*. The full-length mutated DNA was digested with *Pst*I and *Xba*I and subcloned first into the vector pUC19 for sequencing and subsequently into the expression vector pT7.6.

Enzyme Expression and Purification. Wild-type human and mutant inositol monophosphatases were expressed in *Escherichia coli* strain BL21(DE3)pLysS and purified to apparent homogeneity as previously described for the bovine enzyme (Strasser et al., 1995). The concentrations of the purified enzymes were determined from the UV spectra using an extinction coefficient $\epsilon_{280} = 26\,200\ M^{-1}\ cm^{-1}$ (Ganzhorn et al., 1993). Specific activities were 15 units/mg for the the wild-type enzyme and 0.3 units/mg for the K36Q mutant, as determined in a standard assay with 4 mM 2-glycerophosphate and 2 mM $MgCl_2$ at pH 7.5 and 37 °C (Attwood et al., 1988).

Enzyme Assays. Residual activities in all chemical modification experiments were measured in the standard assay (Attwood et al., 1988). Coupled spectrophotometric assay systems (Pelton & Ganzhorn, 1992; Strasser et al., 1995) were used in kinetic experiments with Ins(1)P at pH 7.5 and 37 °C, varying substrates, and metal ions as indicated. For pH dependence studies, a three-component buffer system, consisting of 0.1 M MES, 0.1 M Tris, and 0.033 M CAPS, was used (Ganzhorn & Chanal, 1990). For solvent isotope effects, kinetic constants in H_2O and D_2O were determined at pH 7.5 and 37 °C, using a constant ratio of Tris base and Tris-HCl, as was previously described (Ganzhorn & Chanal, 1990). With glucose 6-phosphate, the release of inorganic phosphate was measured in a discontinuous assay. The enzyme was incubated in 50 mM Tris-HCl, 0.1 mM EGTA, pH 7.5, in the presence of substrate and metal ions, as indicated, in a total volume of 0.5 mL. Aliquots of 100 μL were removed at different time points, and added to 100 μL of a phosphate reagent, in a microtiter plate. The phosphate reagent was prepared by mixing 1 part of 4.2% (w/v) ammonium molybdate (Sigma) in 5 N HCl with 3 parts of 0.2% (w/v) Malachite Green (Merck) in water and adding 0.1% Tween 20 on the day of use (Itaya & Ui, 1966). The absorbance at 600 nm was determined in a plate reader (Dynatech MR5000) and the absorbance change per minute calculated by linear regression. The amount of enzyme was adjusted to maintain a linear response during the time course of the assay. This assay gives similar results as the coupled, continuous systems, but is more reliable in the presence of the higher concentrations of Mg^{2+} that have to be used with this substrate (Strasser et al., 1995). With 4-nitrophenyl phosphate, formation of nitrophenolate was monitored at 400 nm ($\epsilon = 16.7 \times 10^3\ M^{-1}\ cm^{-1}$).

Preparation of Methylated myo-Inositol Monophosphatase for Peptide Mapping. The enzyme (1 mg) in 400 mM triethanolamine hydrochloride, pH 8.0, was incubated at room temperature with 20 mM formaldehyde in the presence of 20 mM sodium cyanoborohydride, 5 mM Ins(1)P, 20 mM lithium chloride, and 10 mM magnesium chloride in a total volume of 2 mL. The reaction was stopped after 60 min by addition of 50 mM lysine. Subsequently, the sample was divided into two parts. The first part was dialyzed against 4-ethylmorpholine acetate buffer, pH 8, and used for enzymatic digestion. The second part was dialyzed against 400 mM triethanolamine hydrochloride, pH 8, to remove lysine and protecting agents. This enzyme was further modified with ^{14}C-labeled formaldehyde (10 mM, 9.8 μCi/μmol) in the presence of 10 mM sodium cyanoborohydride. The reaction was stopped after 75 min, and the enzyme was dialyzed against 4-ethylmorpholine acetate buffer, pH 8, before enzymatic digestion. At various times, 5 μL aliquots were removed, diluted 30-fold into 25 mM Tris-HCl, pH 7.5, with 1 mg/mL bovine serum albumin, and tested for activity.

Glu-C Digestion. Digestion with Glu-C protease from *Staphylococcus aureus* was performed in 0.1 M sodium phosphate buffer, pH 7.8, containing 1 M urea for 20 h using a 10% enzyme/substrate ratio. The enzymatic reaction was stopped by addition of trifluoroacetic acid.

Reverse-Phase Liquid Chromatography (RP-HPLC). Peptides from digests were separated by gradient elution on a

[1] Abbreviations: Ins(1)P, D,L-*myo*-inositol 1-phosphate.

macrobore Waters Delta Pak C18 column (300 Å, 5 μm, 2 × 150 mm) connected to the Applied Biosystems Model 130A syringe pump. The absorbance was monitored at 205 nm using a Model 1000S diode array detector. Solvent A was 0.1% trifluoroacetic acid, and solvent B was 95% acetonitrile/0.1% trifluoroacetic acid. Peptides were eluted using an isocratic step at 2% B for 10 min followed by a gradient starting at 2% B and rising to 70% B in 85 min. Fractions were counted for radioactivity in a BeckmanLS 5000CE liquid scintillation counter or further analyzed by N-terminal sequencing.

N-Terminal Sequencing. N-Terminal sequencing was performed on an Applied Biosystems Model 477A sequencer equipped on-line with a phenylthiohydantoin Model 120A amino acid (PTH-AA) analyzer and a fraction collector. PTH-monomethyllysine was eluted after PTH-leucine, while PTH-dimethyllysine was eluted just after PTH-tyrosine. When sequencing radioactive peptides, one-third of the PTH-AA sample was injected on the analyzer, while the rest was recovered in a collector and counted for radioactivity.

X-ray Structure Determination. Crystals of the K36Q mutant suitable for X-ray structure determination were prepared in the presence of gadolinium sulfate according to the procedure described by Bone et al. (1992). They were isomorphous to the crystals obtained with the wild-type enzyme (space group $P3_221$, $a = b = 86.46$ Å, $c = 154.56$ Å, $\gamma = 120°$, one dimer per asymmetric unit). Diffraction data were collected from one crystal with a Siemens multiwire area detector using graphite-monochromatized Cu Kα radiation produced by an XP18 rotating-anode X-ray generator. The raw data were processed with the program XDS (Kabsch, 1988). A total of 182 288 observations, corresponding to 33 759 unique reflections, were collected to a maximum resolution of 2.20 Å ($R_{sym} = 10.3\%$ on intensities). The data completeness was 97.4% overall and 83.0% in the 2.30−2.20 Å resolution shell (33.8% of the intensities in the higher resolution shell had a signal/noise ratio greater than 2). The crystal coordinates of the wild-type enzyme (Bone et al., 1992; PDB entry 2HHM) were used to obtain initial phases for structure determination. The side-chain atoms of residue 36 were omitted from the calculation of the first difference electron density map. Clear-cut $F_o - F_c$ density (3σ contour above mean) for a glutamine side chain was apparent at position 36 of the polypeptide chain. The structure of the K36Q mutant was subsequently refined by energy minimization with the program X-PLOR version 3.1 (Brunger et al., 1987), using the Engh and Huber force field parameter set (Engh & Huber, 1991). Each cycle of energy minimization was followed by individual isotropic temperature factor refinement. No noncrystallographic symmetry constraints or restraints were applied during refinement. Distances between Gd^{3+} and its potential ligands were not restrained. Water molecules with temperature factors greater than 60 Å^2 were rejected. The final model includes 545 amino acid residues (4A−276A and 5B−276B), 2 Gd^{3+} ions, 2 sulfate ions, and 359 water molecules. The crystallographic *R*-factor is 0.176 for 30 358 unique reflections in the 10.0−2.20 Å resolution shell with amplitudes F greater than $2\sigma(F)$. The final model has acceptable geometry with a rms deviation of 0.006 Å on bond lengths and 1.32° on bond angles.

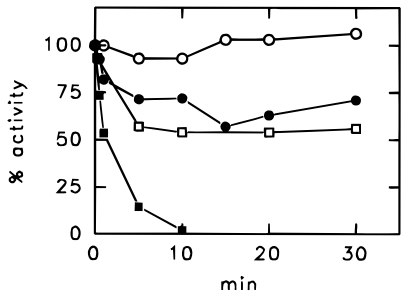

FIGURE 1: Time-dependent inactivation of *myo*-inositol monophosphatase by formaldehyde. 0.05 mg/mL enzyme were incubated in 0.4 M triethanolamine-hydrochloride, pH 8.0, alone (○) or in the presence of 20 mM formaldehyde/cyanoborohydride (■) or 20 mM formaldehyde/cyanoborohydride, 5 mM Ins(1)P, 20 mM LiCl, and 10 mM $MgCl_2$ (□). 0.5 mg/mL of the K36Q mutant enzyme was incubated in the presence of 20 mM formaldehyde/cyanoborohydride (●). Aliquots were removed at the indicated time points and assayed for activity as described under Experimental Procedures.

RESULTS

Chemical Modification. Lysine residues in peptides and proteins are specifically modified by imidoesters to form an amidino group (Pfleiderer, 1985). *myo*-Inositol monophosphatase is completely inactivated by 100 mM or several additions of 20 mM ethyl acetimidate (data not shown). The inhibition is slowed down considerably in the combined presence of Ins(1)P, lithium, and magnesium, a combination that was previously shown to protect active site residues against modification with phenylglyoxal (Jackson et al., 1989), diethyl pyrocarbonate (Pelton & Ganzhorn, 1992), or *N*-ethylmaleimide (Knowles et al., 1992). Despite its high specificity, acetimidate has disadvantages as a modification reagent. Side reactions such as cross-linking of two lysine residues may occur (Browne & Kent, 1975), and labeled imidoesters that would facilitate the identification of active site peptides are not easily obtained. A similar experiment was therefore carried out with formaldehyde as the modification reagent. Lysine residues react with formaldehyde, forming a Schiff base that is subsequently reduced by cyanoborohydride to give stable monomethyllysine. Subsequently, a second methyl group is incorporated to form the tertiary amine, dimethyllysine. In the absence of substrate and metal ions, inositol monophosphatase is completely inactivated by formaldehyde (Figure 1). In contrast, 60% of the initial activity is retained, when Ins(1)P, Li^+, and Mg^{2+} are included in the incubation. No significant protection was detected in the presence of lithium, magnesium, or substrate alone (data not shown).

In order to identify the protected lysine residue(s) responsible for inactivation, the enzyme was first methylated in the presence of protecting agents that were subsequently removed by dialysis. The modified enzyme, with 60% activity as compared to wild-type, was then completely inactivated using ^{14}C-labeled formaldehyde. The amount of radioactivity incorporated corresponded to four dimethylated lysine residues. This result does not allow any conclusions regarding the number of lysine residues in *myo*-inositol phosphatase that are involved in the inactivation process. The different forms of modified enzyme were therefore analyzed in more detail.

Isolation and Characterization of Peptides. Samples obtained before and after the second reductive methylation were digested with Glu-C protease, and soluble peptides were separated by reverse-phase chromatography (Figure 2A,B).

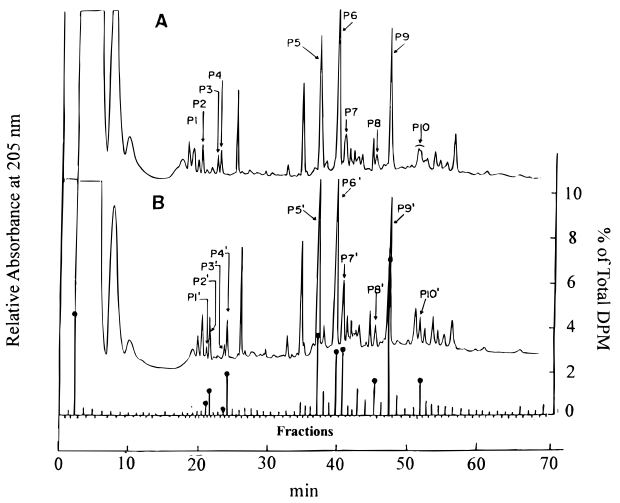

FIGURE 2: RP-HPLC separation of water-soluble peptides generated from endoproteinase Glu-C digests of human *myo*-inositol monophosphatase. (A) Enzyme modified by formaldehyde/cyanoborohydride in the presence of protecting agents. (B) Sample A after removal of protecting agents and a second cycle of modification with [^{14}C]formaldehyde/cyanoborohydride. Labeled peaks were further analyzed by protein sequencing (Table 1). Vertical bars in (B) indicate the relative amount of radioactivity incorporated.

Table 1: Incorporation of Methyl Groups (Me) in Lysine Residues after One (P) or Two (P′) Cycles of Reductive Methylation; P Corresponds to the Peptide Peaks in Figure 2

sequence	HPLC peak	Lys no.	% of methylated forms			av methyl incorporation
			0 Me	1 Me	2 Me	
AA 26−30	P1	28	0	100	0	1.0
	P1′	28	0	84	16	1.2
	P2	28	0	5	95	1.9
	P2′	28	0	0	100	2.0
AA 261−265	P3	264	0	100	0	1.0
	P3′	264	0	97	3	1.0
	P4	264	0	7	93	1.9
	P4′	264	0	5	95	1.9
AA 61−71	P5	61	5	61	34	1.3
	P5′	61	0	46	54	1.5
AA 52−60	P6	52	1	39	60	1.6
	P6′	52	0	49	51	1.5
	P6	59	5	51	44	1.4
	P6′	59	0	24	76	1.8
AA 153−162	P7	156	6	59	35	1.3
	P7′	156	2	33	65	1.6
AA 31−51	P8	36	100	0	0	0
	P8′	36	9	23	68	1.6
	P9	36	88	7	5	0.2
	P9′	36	11	36	53	1.4
	P9	49	1	40	59	1.6
	P9′	49	1	53	46	1.5
AA 78−83	P10	78	41	59	0	0.6
	P10′	78	32	37	32	1.0

Half of the total radioactivity incorporated in the protein was recovered after RP-HPLC in the different fractions. Peaks corresponding to major radioactivity (Figure 2B) were further analyzed by protein sequencing. Since PTH-lysine, PTH-monomethyllysine, and PTH-dimethyllysine were clearly distinguished, we quantitated the number of methyl groups incorporated in a particular lysine residue after the first and the second reductive methylation (Table 1). Apparently, the overall modification with formaldehyde was not complete, as lysine, monomethyllysine, and dimethyllysine were all detected by sequencing. For the hydrophilic peptides AA 26−30 and AA 261−265, the RP-HPLC retention times of the forms containing a monomethyllysine (P1, P′1, P3, and P3′) are slightly higher than the retention times of those that contain a dimethyl lysine (P2, P2′, P4, and P4′). For the other peptides, the different forms were mixed in the same peak. Peptide AA 31−51 was recovered under two peaks (P8 and P9 or P8′ and P9′). The sequences were exactly the same, and the methyl distribution was similar. From mass spectrometry, peaks P8 and P9 appear as a mixture of respectively five and four species differing by 15 ± 1 Da (data not shown). As peptide AA 31−51 contains two lysines (K36 and K49), up to four methyls can be added corresponding to four forms differing by 15 Da. The presence of five forms in peak P8 could be explained by a combination of four methylations and one oxidation of Met-31 or -34 into methionine sulfoxide (+16 Da). This modification cannot be observed by sequencing as it is reduced to methionine by the dithiothreitol present in the reagents. This interpretation is also supported by the fact that peptides containing methionine sulfoxide are usually eluted earlier in RP-HPLC than the corresponding peptide with methionine. Protection against methylation was obvious for Lys-36 in peptides P8 and P9 where respectively 100% and 88% unmodified lysine is still present after the first reductive methylation and only 9% and 11% after the second methylation. For the other peptides, the percentage of different modification states is similar after the first and the second reductive methylation. Finally, Lys-78 seems to be relatively unaccessible to the reagent as 41% and 32% of unmodified lysine is still present after respectively one and two methylation cycles. The relatively high incorporation of methyl during the second cycle of modification is therefore not due to protection during the first cycle, but rather reflects the ongoing modification of a slowly reacting residue.

Peptides containing radioactivity were also analyzed for ^{14}C-labeled amino acids. Only lysine-36 and -78 are significantly radiolabeled, the amount of radioactivity corresponding to 0.8 and 0.6 methyl groups added during the second cycle of modification, while less than 0.3 methyl group was added for lysine residues 28, 49, 52, 59, 61, 156, and 264 (data not shown). Even though the radioactivity measurement gave a lower methyl incorporation for Lys-36, the two methods showed a similar tendency and clearly indicate Lys-36 as the active site residue that was protected during the first modification reaction. The same experiment was performed on bovine *myo*-inositol monophosphatase. The quantity of methyl incorporated during the second modification was only evaluated from the amount of peptide and the incorporation of radioactivity. From sequence analysis, the same peptides as for human *myo*-inositol monophosphatase were radiolabeled with the exception of peptide AA 153−162. Again, Lys-36 was the preferentially radiolabeled amino acid.

Mutagenesis. Lys-36 was replaced with glutamine. The mutation was chosen in order to avoid drastic changes in size or hydrophobicity that may lead to local disruptions of tertiary structure. The specific activity of the purified mutant enzyme in a standard assay was about 2% as compared to wild-type. This activity was not due to a contamination with native enzyme, since it was no longer lost in the presence of formaldehyde (Figure 1). The time course of activity was similar to the situation where wild-type enzyme was modified in the presence of protecting agents. In both cases, residual activities were 50−60% of control levels. This shows that Lys-36 is indeed the active site residue, modification of which, in the absence of protection, leads to inactivation. Second, the decrease in activity in the presence of substrate

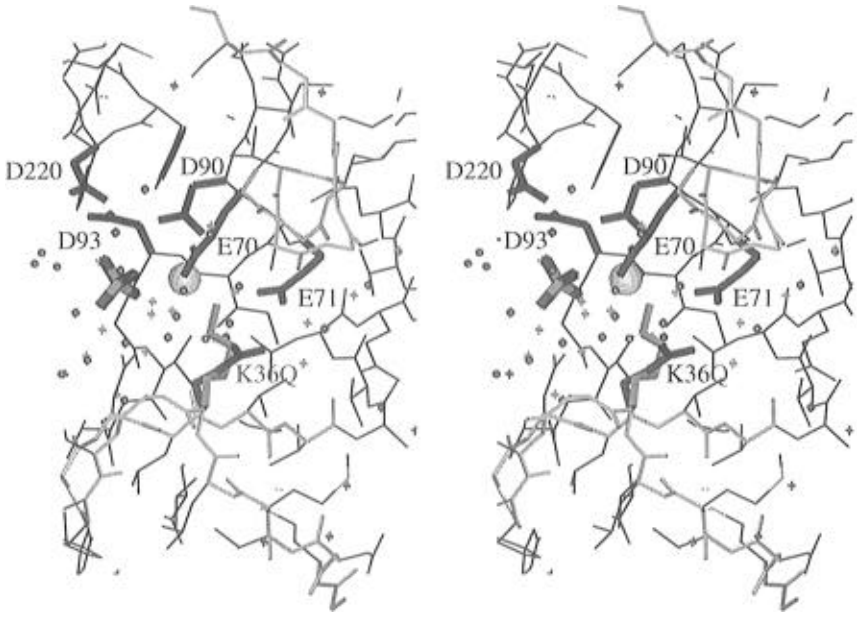

FIGURE 3: Crystal structure of K36Q. The stereoview shows a close-up of the active site, with one Gd^{3+} (large solid sphere) and one sulfate ion bound. The sulfate takes the place of the phosphate moiety in enzyme−substrate complexes (Bone et al., 1994b). The gadolinium ion occupies metal binding site M1, formed by the side chains of E70, D90, and a sulfate oxygen. The side chains of D90, D93, and D220 (shown in boldface) define metal binding site M2. This site is presumably occupied by Li^+, invisible in a protein crystallography experiment. The side chain of the mutated residue, Q36, and the position of the corresponding lysine in the wild-type structure are shown in boldface. In the wild-type enzyme, K36 is involved in a salt bridge interaction with E70 and E71 (also in boldface). These residues belong to two surface protein segments, encompassing residues 30−44 and 70−79 (main chain shown in grey stick representation). The analysis of the structure of the apoenzyme (Bone et al., 1994a) indicates that at least a portion of each of these segments is mobile in the absence of metals and substrate or reaction product. In the K36Q mutant, the water structure around the mutated residue is altered, as indicated by the respective positions of solvent molecules in the mutant (small black spheres) and wild-type structure (gray crosses).

and metal ions is not due to inefficient protection of the active site, but rather caused by the modification of surface residues.

The stability of K36Q with regard to heat denaturation was similar to the native isoform. A transition temperature of 56 °C, as compared to 59 °C for wild-type, was determined in phosphate buffer at pH 7.5 by following the circular dichroism signal at 222 nm (data not shown). The discrepancy in the heat stability as compared to a previous study, where T_m = 87 °C was reported (Ganzhorn et al., 1993), is due to the use of different buffer systems (P. D. Pelton, unpublished experiments). This result indicates that the mutation does not cause any major structural changes.

X-ray Structure Analysis. The X-ray structure of K36Q, crystallized in the presence of sulfate and gadolinium, was determined at 2.20 Å resolution and compared to the crystal structure of the wild-type enzyme, as determined by Bone et al. (1992) under very similar experimental conditions. Lysine-36 is part of a loop region (residues 30−44) which lines the entrance of the enzyme active site. In the mutant structure, there is well-defined electron density for a glutamine residue at position 36 of both monomers (mean isotropic temperature factor for side-chain atoms: 33 $Å^2$ and 47 $Å^2$ for Q36A and Q36B, respectively). Also, the X-ray data show the presence of a sulfate and a gadolinium ion in the enzyme active site, which were also found in the wild-type structure (Bone et al., 1992). Overall, the replacement of lysine-36 by a glutamine does not result in any detectable structural change in the enzyme. The root-mean-square (rms) difference in atomic positions between the wild-type and the K36Q mutant enzyme is 0.20 Å for all main-chain atoms. This is within the expected experimental error at this resolution. It is also very similar to the rms difference (0.27 Å), when the two monomers in the asymmetric unit, refined as independent protein chains, are compared. However, in the mutant structure, the side chain of glutamine-36 is pointing toward the bulk solvent, while lysine-36 in the wild-type structure is directed toward the enzyme active site and makes salt-bridge interactions with both E70 and E71 (Figure 3). This results in a local perturbation of the solvent structure, with two additional water molecules filling up the space previously occupied by the tip of the side chain of lysine-36.

Kinetic Characterization of K36Q. The kinetic constants of K36Q and wild-type enzyme, determined at fixed concentrations of substrate or metal ion, are summarized in Table 2. The mutant enzyme has a 50 times lower turnover number as compared to wild-type, but its substrate K_m is unchanged. Slightly higher concentrations of magnesium are required for activation, whereas no inhibition occurs up to 10 mM of the metal ion. The apparent cooperativity of magnesium activation, seen in the native enzyme (Ganzhorn & Chanal, 1990), is greatly reduced in the mutant form. There are some differences between the data in Table 2 and previously published results. Pollack et al. (1993) found a turnover number of 0.012 s^{-1} for a K36I mutant, but this value was determined at a nonsaturating concentration of Mg^{2+}. The higher K_m for Mg^{2+} activation with K36I (10 mM) may be due to small conformational changes caused by the more hydrophobic side chain.

Several studies have shown that the inositol phosphatase reaction follows an ordered mechanism with one Mg^{2+} binding before Ins(1)P and binding of a second Mg^{2+} to the $E-Mg^{2+}-Ins(1)P$ complex (Leech et al., 1993; Greasley & Gore, 1993; Cole & Gani, 1994; Pollack et al., 1994; Strasser et al., 1995). When the concentration of Mg^{2+} is varied at different fixed levels of the substrate Ins(1)P, data as in Figure 4 are obtained. The main panel shows initial velocities over a wide range of Mg^{2+} concentrations. The

Table 2: Kinetic and Inhibition Constants at pH 7.5 and 37 °C

constant	wild-type	K36Q
k_{cat} (s^{-1})[a]	22 ± 3	0.30 ± 0.03
$A_{0.5}$ (mM)[a]	0.23 ± 0.04	0.80 ± 0.15
n[a]	1.8 ± 0.3	1.1 ± 0.1
K_m (mM)[b]	0.07 ± 0.01	0.020 ± 0.004
$K_{i,Mg}$, (mM)[a]	1.3 ± 0.4	*d*
$K_{i,Li}$ (mM)	0.17 ± 0.01 (K_{ii})[c]	0.84 ± 0.19 (K_{is})[e]
		7.2 ± 0.2 (K_{ii})[e]
$K_{i,Ca}$ (μM)	4.1 ± 0.3 (K_{ii})[c]	9.1 ± 0.4 (K_{ii})[e]

[a] k_{cat} (turnover number), $A_{0.5}$ (the concentration of magnesium giving half-maximal velocity, and n (Hill coefficient) were obtained by varying the concentration of Mg^{2+} over a wide range at 0.5 mM Ins(1)P. Data were fitted by the Hill equation, modified, if required, to account for inhibition at higher concentrations of magnesium: $v = k_{cat}[E][Mg^{2+}]^n/[A_{0.5}{}^n + [Mg^{2+}]^n(1 + [Mg^{2+}]/K_i)]$. [E], the total enzyme concentration, was determined from the UV spectrum (Ganzhorn et al., 1993). [b] Michaelis constant for Ins(1)P, determined at 0.5 and 1 mM Mg^{2+} for the wild-type and mutant enzyme, respectively. [c] From the uncompetitive inhibition patterns in Figure 5 and data analysis using the program UNCOMP (Cleland, 1979). The K_{ii} value for calcium inhibition was corrected for the presence of Mg^{2+} using $K_{ii} = K_{ii,app}/(1 + [Mg^{2+}]/A_{0.5})$ with $A_{0.5} = 0.16$ mM. $K_{ii,Li}$ was not corrected since this corresponds to binding to an enzyme−phosphate complex (Leech et al., 1993) and no competition with the activator magnesium occurs. [d] No inhibition at 10 mM Mg^{2+}. [e] Slope and intercept inhibition constants from the inhibition patterns in Figure 5 and data analysis using the program NONCOMP or UNCOMP (Cleland, 1979). K_{is} and K_{ii} were corrected for the presence of magnesium using $K_{is} = K_{is,app}/(1 + [Mg^{2+}]^2/K_{ia})$ with $K_{ia} = 0.25$ mM^2 and $K_{ii} = K_{ii,app}/(1 + [Mg^{2+}]/K_a)$ with $K_a = 0.65$ mM.

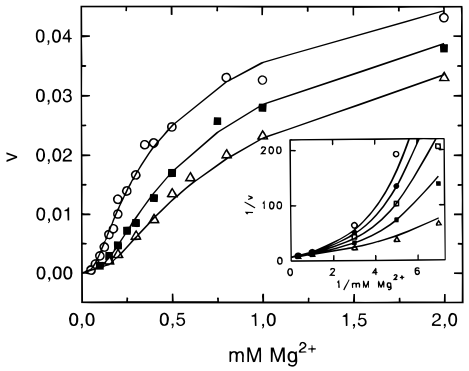

FIGURE 4: Initial velocities with K36Q at pH 7.5 and 37 °C. v has units of ΔA_{360}/min; the enzyme concentration was 0.3 μM. The concentration of Mg^{2+} was varied at different fixed levels of Ins(1)P: 0.056 (△), 0.071 (■), and 0.5 mM (○). Inset: Double-reciprocal plot of a similar experiment with 0.8 μM enzyme and Ins(1)P concentrations of 0.056 (○), 0.071 (●), 0.1 (□), 0.167 (■), and 0.5 mM (△). The lines in both graphs are from an overall fit of the data by eq 2.

inset shows a plot of $1/v$ versus $1/[Mg^{2+}]$ for a different experiment at five fixed concentrations of substrate and Mg^{2+} concentrations close to saturation. Visual inspection of the latter indicates that the lines may intersect in a common point on the $1/v$ axis. Consequently, the data were also analyzed for each substrate concentration separately by using the Hill equation: $v = V[Mg^{2+}]^n/(K_a{}^n + [Mg^{2+}]^n)$. There was no statistically significant difference in V (and therefore the intercept in the inset to Figure 4) for any two substrate concentrations, as shown by Student's t test. The replot of $1/v$ versus 1/[Ins(1)P] of the same data (not shown) gave a series of straight lines, which clearly did not intersect in a common point on the $1/v$ axis, but their slopes approached zero at the highest concentrations of Mg^{2+}. These observations taken together are consistent with a rapid equilibrium ordered mechanism with one metal ion binding after the substrate (Segel, 1975). The switch from the sequential pattern for the wild-type enzyme (Leech et al., 1993) to the rapid equilibrium ordered pattern for K36Q is explained by the drop in k_{cat}: since the binding of substrate and metal ions is basically unchanged in the mutant, their rate of dissociation may now be fast as compared to the rate of catalysis.

Table 3: Rapid Equilibrium Kinetic Constants for K36Q at pH 7.5 and 37 °C

	2 metals		3 metals	
constant[a]	expt 1[b]	expt 2[c]	expt 1[b]	expt 2[c]
k_{cat} (s^{-1})	0.25 ± 0.01	0.29 ± 0.01	0.25 ± 0.01	0.27 ± 0.01
K_{ia} (mM)	0.87 ± 0.49	18 ± 47		
K_{ia} (mM^2)			0.12 ± 0.04	0.25 ± 0.05
K_a (mM)	0.61 ± 0.08	0.53 ± 0.06	0.64 ± 0.07	0.65 ± 0.06
K_b, (mM)	0.04 ± 0.01	0.01 ± 0.01	0.06 ± 0.01	0.04 ± 0.01
χ^2	3.3×10^{-6}	1.10×10^{-5}	2.0×10^{-6}	1.05×10^{-5}

[a] Initial velocities of both experiments in Figure 4 were fitted by eq 1 (2 metal ions; $K_{ia} = E{\cdot}A/EA$, $K_b = EA{\cdot}B/EAB$, and $K_a = EAB{\cdot}A/EABA$) or eq 2 (3 metal ions; $K_{ia} = E{\cdot}A^2/EA_2$, $K_b = EA_2{\cdot}B/EA_2B$, and $K_a = EA_2B{\cdot}A/EA_2BA$). χ^2 is the sum of squares of the residuals. [b] Data from main panel, Figure 4. [c] Data from inset to Figure 4.

Initial velocity patterns of IMPase have previously been analyzed using an approximation based on the Hill equation (Strasser et al., 1995). Applying the rapid equilibrium assumption, a more realistic model, based on the enzymatic mechanism, can be derived for K36Q. The mechanism with one metal ion binding before and a second metal ion after the substrate is described by eq 1 (Segel, 1975):

$$V_{max}/v = K_{ia}K_bK_a/A^2B + K_bK_a/AB + K_a/A + 1 \quad (1)$$

where A and B are the concentrations of magnesium and substrate, respectively, $K_{ia} = E{\cdot}A/EA$, $K_b = EA{\cdot}B/EAB$, and $K_a = EAB{\cdot}A/EABA$ (E is the concentration of free enzyme). The equation correctly predicts the common $1/v$ intercept, when varying the metal ion at constant substrate concentrations. It also predicts that the apparent cooperativity of magnesium activation, determined by the square term in eq 1, should disappear when the substrate B becomes saturating. When the data in Figure 4 (or the inset to Figure 4) are analyzed separately using the Hill equation, the Hill coefficients indeed decrease from around $n = 2$ [at 0.056 mM Ins(1)P] to $n = 1.1$ [at 0.5 mM Ins(1)P]. With wild-type enzyme, no such trend is observed, and the Hill coefficient stays at 2 even at saturating concentrations of substrate (Table 2). When the data set of Figure 4 (main panel) was analyzed using eq 1, the fitting process converged to the parameters shown in Table 3, with a large standard error for K_{ia}. Fitting eq 1 to the data of the inset to Figure 4 gave a different set of parameters with very high standard errors for K_{ia} and K_b (Table 3). Obviously, eq 1 is not a good description for the data in Figure 4.

Recent structural studies have indicated that up to three metal ion binding sites are present in the active site of IMPase (Bone et al., 1994a). Since only two metals remain in the complex with reaction products, the third one had not been implicated in catalysis. We have considered a third catalytic metal ion to see whether a better fit of the kinetic data may be obtained. For the nonlinearity of magnesium activation to disappear at saturating substrate levels, two of the three metals must bind before the substrate (Scheme 1). Using the rapid equilibrium assumption, eq 2 can be derived for the mechanism in Scheme 1, lower pathway. E was assumed

Scheme 1: Proposed Kinetic Mechanism of *myo*-Inositol Monophosphatase: Ester Hydrolysis and Dissociation of the Alcohol and the Third Metal Ion Are Combined in One Step

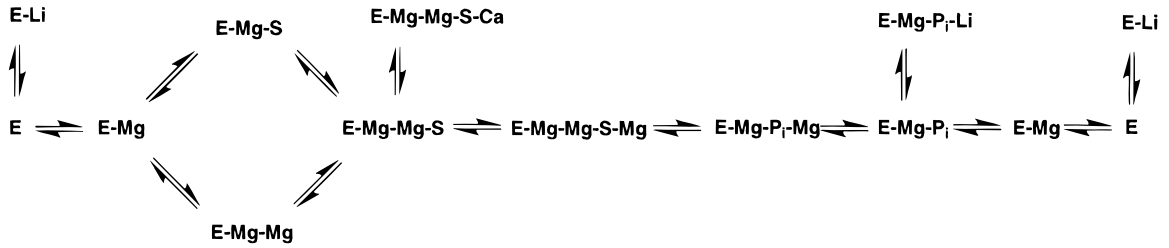

to directly combine with 2 Mg^{2+} to give EA_2:

$$V_{max}/v = K_{ia}K_bK_a/A^3B + K_bK_a/AB + K_a/A + 1 \quad (2)$$

where $K_{ia} = E{\cdot}A^2/EA_2$, $K_b = EA_2{\cdot}B/EA_2B$, and $K_a = EA_2B{\cdot}A/EA_2BA$. Again, the equation correctly predicts the qualitative observations regarding $1/v$ intercepts and apparent cooperativity. In addition, a better fit to the data and realistic and reproducible parameters are obtained for both experiments (Figure 4 and Table 3). The K_b value for substrate binding is slightly higher than the K_m in Table 2 as a consequence of the rapid equilibrium ordered mechanism. K_a, the binding constant for the third metal ion, is in good agreement with $A_{0.5}$ in Table 2. It appears that the binding of the last (third) magnesium ion is somewhat weaker than in the wild-type enzyme, but this could be a consequence of the inhibitory action of magnesium in the wild-type enzyme, which may perturb the correct data analysis. In summary, eq 2 is a better description of the experimental data than eq 1, since it provides parameters which are independent of the concentration range that is analyzed and have smaller errors and smaller sum of residual squares. It should be noted that eq 2 predicts highly cooperative binding of the first two Mg^{2+} ions. In other words, the first Mg^{2+} favors binding of the second to form $E-Mg^{2+}-Mg^{2+}$, and $E-Mg^{2+}$ does not occur to a significant extent. A priori, this was not an unreasonable assumption, since the two metal ions are very close and share at least one ligand, namely, Asp-90 (see Discussion and legend to Figure 3). However, equations based on models with independent binding of the first two metal ions (not shown), either in a random or in an ordered fashion, give rise to fits that are almost as good as with eq 2 (and always better than eq 1). Therefore, our data do not yield any information on the mode of binding of the first two metal ions.

Inhibition of the K36Q mutant by lithium and calcium was studied and compared to the native human enzyme (Table 2 and Figure 5). Calcium is equally potent with both enzyme forms and acts as an uncompetitive inhibitor (Figure 5A,B). Lithium, on the other hand, is uncompetitive only with the wild-type enzyme, whereas with K36Q the mechanism of inhibition becomes noncompetitive and the inhibitory potency drops by an order of magnitude (Figure 5C,D).

pH Dependence Studies. It was previously recognized that activation of bovine inositol monophosphatase by Mg^{2+} greatly depends on pH (Ganzhorn & Chanal, 1990). Maximal rates therefore have to be determined by simultaneously varying the concentrations of substrate and metal ion at each pH value. The pH dependence of catalysis for the K36Q mutant enzyme was studied between pH 7.0 and 9.5. V_{max} was determined from fitting with eq 2 and log k_{cat} plotted against pH (Figure 6). The wild-type enzyme was studied over the range of pH 6.0−8.5. In this case, the rapid

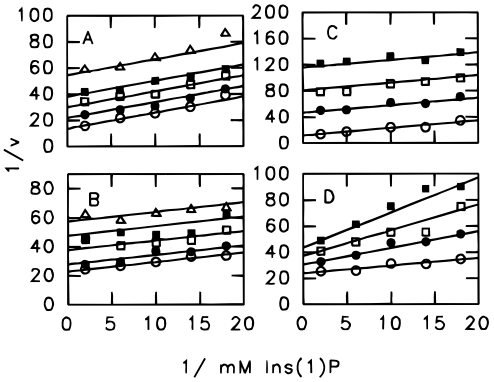

FIGURE 5: Inhibition of wild-type and mutant *myo*-inositol monophosphatase by calcium and lithium. (A) Inhibition of wild-type enzyme (7 nM) by Ca^{2+} [0 (○), 10 (●), 20 (□), 30 (■), and 50 (△) μM] at 0.5 mM Mg^{2+}. The lines were calculated from a fit with the program UNCOMP, with $V = 0.074 \pm 0.002$, $K_m = 0.090 \pm 0.006$ mM, and $K_{ii} = 16 \pm 1$ μM. (B) Inhibition of K36Q (300 nM) by Ca^{2+} [0 (○), 5 (●), 15 (□), 25 (■) and 35 (△) μM] at 1 mM Mg^{2+}. Fitting with UNCOMP gave $V = 0.044 \pm 0.001$, $K_m = 0.029 \pm 0.004$ mM, and $K_{ii} = 23 \pm 1$ μM. (C) Inhibition of wild-type enzyme (9 nM) by Li^+ [0 (○), 0.5 (●), 1 (□), and 1.5 (■) mM] at 0.5 mM Mg^{2+}. Fitting with UNCOMP gave $V = 0.083 \pm 0.002$, $K_m = 0.095 \pm 0.007$ mM, and $K_{ii} = 0.17 \pm 0.01$ mM. (D) Inhibition of K36Q (300 nM) by Li^+ [0 (○), 5 (●), 10 (□) ,and 15 (■) mM] at 1 mM Mg^{2+}. Fitting with NONCOMP gave $V = 0.042 \pm 0.001$, $K_m = 0.024 \pm 0.004$ mM, $K_{is,app} = 4.2 \pm 1.0$ mM, and $K_{ii,app} = 18.1 \pm 2.6$ mM. v has units of ΔA_{360}/min.

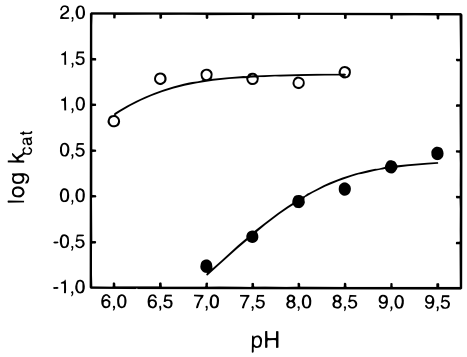

FIGURE 6: pH dependence of k_{cat} for wild-type *myo*-inositol monophosphatase (○) and the K36Q mutant enzyme (●). Turnover numbers at different pH values were determined by fitting initial velocity data with eq 2. The curves for the pH profiles were calculated from a fit to log (k_{cat}) = log ($k_{cat,max}$) − log ($1 + 10^{pK-pH}$). For wild-type enzyme, $k_{cat,max}$ was 22 ± 3 s^{-1} and p$K = 6.2 \pm 0.2$. For K36Q, $k_{cat,\ max}$ was 2.5 ± 0.4 and p$K = 8.2 \pm 0.1$.

equilibrium assumption is only valid at low pH values (Leech et al., 1993), and eq 2 may not correctly describe the data over the whole pH range. However, V_{max} was not very sensitive with respect to different models used for data analysis, and eq 2 was also applied to the wild-type enzyme. Figure 6 shows that k_{cat} is pH-independent for wild-type *myo*-inositol monophosphatase at least between pH 7 and 8.5, but drops at acidic pH values. This result is in agreement

Table 4: Substrate Specificity of Wild-Type and Mutant *myo*-Inositol Monophosphatase at pH 7.5 and 37 °C

	k_{cat} (s^{-1})		
	Ins(1)P[a]	D-glucose 6-phosphate[b]	4-nitrophenyl phosphate[b]
wild-type	22	1.6	0.6
K36Q	0.3	0.2	0.6

[a] From Table 2. [b] Apparent maximal velocities (V_{app}) were first determined by varying substrate concentrations at different fixed levels of Mg^{2+}. Maximal velocities were determined from a replot of V_{app} versus Mg^{2+} concentration, and k_{cat} was calculated taking into account the total enzyme concentration.

with previously published data on the bovine enzyme (Ganzhorn & Chanal, 1990; Leech et al., 1993). In contrast, K36Q displays a clear pH dependence for k_{cat} over the whole range between pH 7 and 9. The curve may have an inflection point at pH 8.2. However, since reliable kinetic data could not be obtained above pH 9.5, we do not know whether a plateau is reached or k_{cat} further increases at higher pH.

Solvent Isotope Effects. Kinetic constants were also determined in H_2O and D_2O. For wild-type enzyme, solvent isotope effects were $^{D}V = 2.4$ and $^{D}V/K = 1.3$, similar to the results with the bovine enzyme (Ganzhorn & Chanal, 1990). For K36Q, ^{D}V was 1.4, and $^{D}V/K$ was 1.0.

Substrate Specificity. D-Glucose 6-phosphate and 4-nitrophenyl phosphate are weak substrates of bovine *myo*-inositol monophosphatase with 10−20-fold lower turnover numbers as compared to Ins(1)P (Strasser et al., 1995). The same substrates were tested with the human enzyme as well as K36Q, and turnover numbers are summarized in Table 4. Whereas the wild-type enzyme is clearly selective for Ins(1)P, the mutant form does not distinguish between the three substrates, at least with respect to their maximal rate of cleavage. The structure of the alcohol moiety, an important factor in the catalytic mechanism of *myo*-inositol phosphatase (Attwood et al., 1988; Baker et al., 1989), obviously no longer affects catalysis by K36Q.

DISCUSSION

Accessible surface lysine residues in *myo*-inositol monophosphatase can be modified by formaldehyde with only minor loss of enzyme activity. The active site is protected from modification in the combined presence of substrate and metal ions, but complete inactivation occurs upon modification of the active site residue, Lys-36. A mutant enzyme, K36Q, confirms the results from the chemical modification study. It has a 50-fold reduced turnover number as compared to wild-type enzyme, but unchanged affinity for the substrate, and turned out to be a very useful tool to study the enzymatic mechanism of *myo*-inositol monophosphatase.

Lithium, calcium, and magnesium are uncompetitive inhibitors of the inositol phosphatase reaction (Hallcher & Sherman, 1980; Ganzhorn & Chanal, 1990; Strasser et al., 1995). Lithium inhibits preferentially by binding to a $E-Mg^{2+}-P_i$ complex (Scheme 1), thereby preventing the dissociation of inorganic phosphate (Leech et al., 1993). The K_i value of Li^+ inhibition is therefore an apparent dissociation constant, which depends on the steady-state concentration of $E-Mg^{2+}-P_i$. Mutant enzymes with low turnover numbers and rate-limiting ester hydrolysis should then no longer be inhibited by lithium, since the enzyme−phosphate complex does not accumulate (Pollack et al., 1993). Indeed, the efficiency of lithium inhibition of K36Q is greatly reduced, and the pattern becomes noncompetitive. The K_{is} value of about 1 mM most likely corresponds to lithium binding to free enzyme, whereas the K_{ii} of about 7 mM reflects binding to an enzyme−substrate complex. These values are in excellent agreement with slope and intercept inhibition constants from a complementary experiment with wild-type enzyme, but using a slow substrate, 4-nitrophenyl phosphate (Strasser et al., 1995). This also indicates that lithium inhibition of K36Q is not reduced because of a direct effect of the mutation on metal ion binding, but rather the indirect effect of the slow turnover number. Magnesium, at high concentrations, is also an uncompetitive inhibitor of wild-type *myo*-inositol monophosphatase, mutually exclusive with lithium (Ganzhorn & Chanal, 1990). Similar to Li^+, it binds to $E-Mg^{2+}-P_i$, trapping the enzyme on the level of the $E-Mg^{2+}-P_i-Mg^{2+}$ complex (Leech et al., 1993; Scheme 1). Again, since $E-Mg^{2+}-P_i$ does not accumulate in low turnover mutants, these should no longer be inhibited by excess Mg^{2+}. This is clearly demonstrated in the case of K36Q, which is efficiently activated by low concentrations of Mg^{2+}, but not inhibited by up to 10 mM of the metal ion. Calcium, on the other hand, binds to enzyme−substrate complexes, inhibiting substrate hydrolysis, and displays a particularly high affinity for $E-Mg^{2+}-$Ins(1)P (Strasser et al., 1995). Calcium inhibition is consequently unaffected by the K36Q mutation with respect to potency and mechanism. These results confirm our previous suggestion (Strasser et al., 1995) that different metal ions exert their inhibitory effects through binding to different enzyme forms (Scheme 1).

There is general agreement now that the nonlinear kinetics of Mg^{2+} activation, first shown by Ganzhorn and Chanal (1990), are due to the requirement for more than one metal ion for substrate binding and catalysis, with one Mg^{2+} binding before and a second after the substrate (Greasley & Gore, 1993; Cole & Gani, 1994; Pollack et al., 1994; Strasser et al., 1995). Certain kinetic data, however, are difficult to reconcile with a two metal ion mechanism. Saturating concentrations of the substrate should trap the first Mg^{2+} ion, causing the nonlinearity of metal activation to disappear. This is not the case, since sigmoidal activation curves (Hill coefficient > 1) are found in the presence of saturating Ins(1)P [Table 2 and Ganzhorn and Chanal (1990)], 4-nitrophenyl phosphate (Strasser et al., 1995), and 2′-AMP (but not inositol 4-phosphate; Leech et al., 1993). One may argue that the first metal ion can dissociate, leaving E−Ins(1)P. However, the existence of an enzyme−substrate complex in the absence of metal ions can be ruled out almost with certainty. First, phosphate only binds to the enzyme in the presence of Mg^{2+} (Greasley & Gore, 1993); second, Ins(1)P or an inhibitory substrate analog does not perturb the fluorescence of pyrenylmaleimide-labeled enzyme (Greasley et al., 1994); and third, significant protection against chemical modification or proteolysis was found only in the presence of metal ions, but never with substrate alone [this study and Jackson et al. (1989), Gee et al. (1991), and Pelton and Ganzhorn (1992)]. In addition, given the high number of negatively charged residues surrounding the phosphate binding pocket (Bone et al., 1992), it seems impossible that a phosphate anion may bind without being ligated to a cation. With the K36Q mutant, cooperativity seems to disappear with increasing concentrations of substrate, but still, the analysis of the initial velocity data indicates that more than two metal

ions are involved in catalysis. We therefore propose the mechanism in Scheme 1 as being compatible with the kinetic data, collected by us and by others. K36Q would then mainly follow the lower pathway with two Mg^{2+} being trapped by the substrate. In contrast, the upper pathway would become significant with the wild-type enzyme: cooperativity does not disappear with saturating Ins(1)P, since the second metal ion can dissociate from the E−Mg^{2+}−Mg^{2+}−S complex. The switch from a more random to an ordered mechanism in K36Q may be attributed to the removal of a positive charge, which, in the wild-type enzyme, facilitates dissociation of one Mg^{2+} from E−Mg^{2+}−Mg^{2+}−S.

Previously, a three metal ion mechanism was ruled out based on the X-ray structure of the enzyme complexed to inorganic phosphate and two manganese ions (Bone et al., 1994a). However, this structure may not be conclusive with respect to the situation in the enzyme−substrate complex, since a third metal ion may dissociate after ester cleavage and no longer be found in an enzyme−phosphate complex. Interestingly, a structure of the enzyme complexed to manganese in the absence of substrate or product shows three metal ion binding sites (Bone et al., 1994a), as did binding studies with ^{45}Ca (Pollack et al., 1994). Recently, we have also observed an X-ray structure of an enzyme−Ins(1)P complex, which clearly shows the presence of three calcium ions at the same sites as the three Mn^{2+} ions in the enzyme−Mn^{2+} complex (J.-M. Rondeau, unpublished data). On a molecular basis, it was proposed (Bone et al., 1994a; Pollack et al., 1994) that one Mg^{2+}, binding to metal site M1, which corresponds to the Gd^{3+} site in Figure 3, activates a water molecule for nucleophilic attack on the phosphate ester, whereas a second Mg^{2+} at site M2, which is ligated by Asp-93, Asp-90, and Asp-220 (Figure 3), stabilizes the alcoholate leaving group. This may also be the inhibitory lithium binding site (Pollack et al., 1994). Alternatively, the hydrolytic water may be activated by the second Mg^{2+}, leading to an adjacent associative displacement of the alcohol (Wilkie et al., 1995). The third metal ion (site M3) is also ligated to Glu-70 and to one of the phosphate oxygens (Bone et al., 1994a; J.-M. Rondeau, unpublished results). Calcium, an uncompetitive inhibitor versus substrate and competitive versus Mg^{2+} (Strasser et al., 1995), may bind to site M3, as proposed in Scheme 1.

Lys-36 interacts with Glu-70, a ligand of metal ion M1 (and M3). It was hypothesized in a previous site-directed mutagenesis study that replacement of Lys-36 with isoleucine alters the active site of *myo*-inositol monophosphatase structurally or electrostatically (Pollack et al., 1993). Major structural perturbations in our K36Q mutant are ruled out by the X-ray data and the fact that substrate recognition and binding of metal ions to any site are all but slightly altered. Assuming that Mg^{2+} at site M1 activates the water nucleophile, it would do so by lowering its pK_a, such that a significant amount of $Mg(OH)^+$, which is a much better nucleophile than water itself, can be formed at neutral pH (Herschlag & Jencks, 1990). The pK_a of Mg^{2+}-bound water is 12.6 in free solution (Herschlag & Jenks, 1990), but in an enzyme active site depends on the nature of the other metal ligands. From this point of view, activation by Mg^{2+} at M1 may not be very efficient, given the interaction with the negatively charged phosphate and two carboxylates (Figure 3). Lys-36, through its interaction with the carboxyl group of Glu-70, reduces the negative charge to which the metal ion is exposed. Consequently, it should increase its polarizing potential and facilitate deprotonation of the water nucleophile. In addition, the pK value of 6.2 for k_{cat}, still too low for Mg^{2+}-bound water, indicates that formation of the active nucleophile is further aided by base-catalysis, consistent with a solvent isotope effect of 2 (Ganzhorn & Chanal, 1990). Removal of K36 and its polarizing charge appears to decrease the efficiency of proton transfer, as reflected by the low rate of catalysis, the shift in the pH dependence of k_{cat}, and the reduced solvent isotope effect in the K36Q mutant enzyme.

It is not immediately clear how this hypothesis could explain the observation that substrates having quite different turnover numbers with the wild-type enzyme are hydrolyzed at similar rates by the K36Q mutant. This may only be possible if the alcohol part of the substrate itself is involved in the activation of the water nucleophile. Such a mechanism was recently put forward by Wilkie et al. (1995), who suggested that the hydrolytic water molecule is actually bound to the metal ion at M2 and held in place by the so-called "catalytic" oxygen functionality [the 6-hydroxyl group in D-Ins(1)P (Baker et al., 1989)] of the substrate. On the other hand, there is no indication from the X-ray structure for any, even indirect, interaction between K36 and Mg^{2+} at site M2. Our suggestion of a third metal ion being involved in catalysis may solve this apparent contradiction. This metal ion is also ligated to E70 (Bone et al., 1994a; Jean-Michel Rondeau, unpublished results) and most likely in a position to activate a water molecule, which also interacts with a substrate hydroxyl. Any conclusion made above for the interaction between K36 and M1 would also apply to M3. In addition, in a mutant enzyme, such as K36Q, where this interaction and its activating effect on the water nucleophile are perturbed, substrate hydroxyl groups may no longer be able to further aid in catalysis. Consequently, similar, low turnover numbers are found for different substrates, whether or not they possess the catalytic hydroxyl group, and only a synergistic effect of K36 and a substrate oxygen leads to full catalytic activity.

An electrostatic effect, which increases the polarizing potential of a catalytic metal ion, appears altogether sufficient to rationalize the role of K36 in catalysis. However, a second explanation of its role and for the changes in kinetic parameters, seen in the K36Q mutant enzyme, may be considered. At least two segments in the three-dimensional structure of *myo*-inositol monophosphatase, lining the entrance to the active site, appear to undergo conformational changes upon substrate and metal ion binding. One of them, comprising residues 30−40, becomes completely disordered in the apoenzyme, whereas the other, comprising residues 70−75, moves away from the cation binding site (Bone et al., 1994a; and Figure 3). If these two loops have to approach each other for catalysis to occur, the chemical step in Scheme 1 would have to be expanded as follows:

Scheme 2

$$E1 \underset{k_{-c}}{\overset{k_c}{\rightleftharpoons}} E2 \xrightarrow{k_H} E3$$

where E1 = E−Mg^{2+}−Mg^{2+}−S−Mg^{2+}, E2 = E*−Mg^{2+}−Mg^{2+}−S−Mg^{2+}, and E3 = E*− Mg^{2+}−Mg^{2+}−P_i; k_c, k_{-c}, and k_H are the rate constants for loop movement and hydrolysis. There is no hint from the X-ray structure of K36Q that loop closure is disturbed in the mutant enzyme.

Both flexible segments are fixed in a position undistinguishable from the corresponding wild-type structure. However, it should be pointed out that these two segments are involved in crystal packing interactions with symmetry-related molecules, which may mask a change in mobility. This is in contrast to the situation in apo-enzyme crystals, which belong to a different crystal form, and where mobility is observed. Nevertheless, the mutation may affect the rate of loop movement that leads to the structure shown in Figure 3, since K36, through strong salt bridge interactions with E70 and E71, provides an anchoring point to hold the two segments together or at least facilitate their approach. A decrease in k_c (Scheme 2) in the mutant enzyme could cause a change in the rate-limiting step from hydrolysis to loop movement. This would be an alternative explanation, why substrates with different turnover numbers in the wild-type enzyme, where ester hydrolysis is rate-limiting (Ganzhorn & Chanal, 1990), are cleaved at similar rates by K36Q. A rate-limiting conformational change would also produce an internal commitment factor (Cook & Cleland, 1981) leading to the reduced isotope effect (Northrop, 1992).

Even though a perturbation of segment movement in the K36Q mutant cannot be ruled out, it remains somewhat speculative in the absence of more direct evidence. The modified electrostatic environment in the active site, however, is a reality, which favors the latter as an explanation for the observed changes in the kinetic parameters of the K36Q mutant enzyme. In conclusion, we have shown that methylation of Lys-36 in *myo*-inositol monophosphatase, or its mutation to glutamine, is detrimental to catalytic activity. The low turnover number of the mutant enzyme and other modifications to catalytic parameters are not due to structural changes. Rather, Lys-36, through its charge interaction with a glutamic acid residue, increases the polarizing potential of one of the catalytic metal ions. This in turn facilitates proton transfer from the metal-bound nucleophile to a nearby base. The identity of this base is presently still unclear, as is the question, which of the metal ions carries the nucleophilic water molecule. Some of the data presented in this paper however indicate that a newly identified catalytic magnesium ion at site M3 may play this role. More X-ray structures with substrates and metal ions are presently analyzed that will hopefully provide answers to the remaining questions.

REFERENCES

Attwood, P. V., Ducep, J. B., & Chanal, M. C. (1988) *Biochem. J. 253*, 387.

Baker, R., Kulagowski, J. J., Billington, D. C., Leeson, P. D., Lennon, I. C., & Liverton, N. J. (1989) *J. Chem. Soc., Chem. Commun.*, 1383.

Belmaker, R. H., Bersudsky, Y., Benjamin, J., Agam, G., Levine, J., & Kofman, O. (1995) in *Depression and Mania: From Neurobiology to Treatment* (Gessa, G., Fratta, W., Pani, L., & Serra, G., Eds.) pp 67−84, Raven Press, New York.

Berridge, M. J., Downes, C. P., & Hanley, M. R. (1989) *Cell 59*, 411.

Bone, R., Springer, J. P., & Atack, J. R. (1992) *Proc. Natl. Acad. Sci. U.S.A. 89*, 10031.

Bone, R., Frank, L., Springer, J. P., & Atack, J. R. (1994a) *Biochemistry 33*, 9468.

Bone, R., Frank, L., Springer, J. P., Pollack, S. J., Osborne, S., Atack, J. R., Knowles, M. R., McAllister, G., Ragan, C. I., Broughton, H. B., Baker, R., & Fletcher, S. R. (1994b) *Biochemistry 33*, 9460.

Browne, D. T., & Kent, S. B. H. (1975) *Biochem. Biophys. Res. Commun. 67*, 126.

Brunger, A. T., Kuriyan, J., & Karplus, M. (1987) *Science 235*, 458.

Cleland, W. W. (1979) *Methods Enzymol. 63*, 103.

Cole, A. G., & Gani, D. (1994) *J. Chem. Soc., Chem. Commun.*, 1139.

Cook, P. F., & Cleland, W. W. (1981) *Biochemistry 20*, 1797.

Engh, R. A., & Huber, R., (1991) *Acta Crystallogr. A47*, 392.

Gani, D., Downes, C. P., Batty, I., & Bramham, J. (1993) *Biochim. Biophys. Acta 1177*, 253.

Ganzhorn, A. J., & Chanal, M. C. (1990) *Biochemistry 29*, 6065.

Ganzhorn, A. J., Vincendon, P., & Pelton, J. T. (1993) *Biochim. Biophys. Acta 1161*, 303.

Gee, N. S., Knowles, M. R., McAllister, G., & Ragan, C. I. (1991) *FEBS Lett 284*, 95.

Gore, M. G., Greasley, P., McAllister G., & Ragan, C. I. (1993) *Biochem. J. 296*, 811.

Greasley, P. J., & Gore, M. G. (1993) *FEBS Lett. 331*, 114.

Greasley, P. J., Hunt, L. G., & Gore, M. G. (1994) *Eur. J. Biochem. 222*, 453.

Hallcher, L. M., & Sherman, W. R. (1980) *J. Biol. Chem. 255*, 10896.

Herschlag, D., & Jencks, W. P. (1990) *Biochemistry 29*, 5172.

Ho, S. N., Hunt, H. D., Horton, R. M., Pullen, J. K., & Pease, L. R. (1989) *Gene 77*, 51.

Itaya, K., & Ui, M. (1966) *Clin. Chim. Acta 14*, 361.

Jackson, R. G., Gee, N. S., & Ragan, C. I. (1989) *Biochem. J. 264*, 419.

Jope, R. S., & Williams, M. B. (1994) *Biochem. Pharmacol. 47*, 429.

Kabsch, W. (1988) *J. Appl. Crystallogr. 21*, 916.

Knowles, M. R., Gee, N. S., McAllister, G., Ragan, C. I., Greasley, P. J., & Gore, M.G. (1992) *Biochem. J. 285*, 461.

Leech, A. P., Baker, G. R., Shute, J. K., Cohen, M. A., & Gani, D. (1993) *Eur. J. Biochem. 212*, 693.

McAllister, G., Whiting, P., Hammond, E. A., Knowles, M. R., Atack, J. R., Bailey, F. J., Maigetter, R., & Ragan, C. I. (1992) *Biochem. J. 284*, 749.

Nahorski, S. R., Ragan, C. I., & Challiss, R. A. J. (1991) *Trends Pharmacol. Sci. 12*, 297.

Northrop, D. B. (1982) *Methods Enzymol. 87*, 607.

Parthasarathy, L., Vadnal, R. E., Parthasarathy, R., & Devi, C. S. S. (1994) *Life Sci. 54*, 1127.

Pelton, P. D., & Ganzhorn, A. J. (1992) *J. Biol. Chem. 267*, 5916.

Pfleiderer, G. (1985) in *Modern Methods in Protein Chemistry* (Tschesche, H., Ed.) Vol. 2, pp 207−259, Walter de Gruyter, Berlin.

Pollack, S. J., Knowles, M. R., Atack, J. R., Broughton, H. B., Ragan, C. I., Osborne, S., & McAllister, G. (1993) *Eur. J. Biochem. 217*, 281.

Pollack, S. J., Atack, J. R., Knowles, M. R., McAllister, G., Ragan, C. I., Baker, R., Fletcher, S. R., Iversen, L. L., & Broughton, H. B. (1994) *Proc. Natl. Acad. Sci. U.S.A. 91*, 5766.

Rees-Milton, K. J., Greasley, P. J., Ragan, C. I., & Gore, M. G. (1993) *FEBS Lett. 321*, 37.

Segel, I. H. (1975) in *Enzyme Kinetics*, pp 242−272, John Wiley & Sons, New York.

Strasser, F., Pelton, P. D., & Ganzhorn, A. J. (1995) *Biochem. J. 307*, 585.

Wilkie, J., Cole, A. G., & Gani, D. (1995) *J. Chem. Soc., Perkin Trans. 1*, 2709.

Wreggett, K. A. (1992) *Biochem. J. 286*, 147.

BI9603837